FOREX Publication
Open Access | Rapid and quality publishing

International Journal of
Electrical and Electronics Research (IJEER)
Research Article | Volume 14, Issue 1 | Pages 1-9 | e-ISSN: 2347-470X

Miniaturized Wearable Antenna Design for Wireless Body Area Networks at 5.8 GHz

Sivasankari Narasimhan[1*] Ashwini G[2], and Karthika K[3]

[1]*Department of Electronics and Communication Engineering, Mepco Schlenk Engineering College, Anna University, India; Email: sivasankari2015@mepcoeng.ac.in*
[2]*Department of Electronics and Communication Engineering, Mepco Schlenk Engineering College, Anna University, India; Email: ashwinig162001_ec@mepcoeng.ac.in*
[3]*Department of Electronics and Communication Engineering, Mepco Schlenk Engineering College, Anna University, India; Email: karthikakannan2000kvp_ec@mepcoeng.ac.in*

***Correspondence:** *sivani.sivasankari@gmail.com; Tel.: +91-8870709780*

ABSTRACT- Microstrip patch antennas are extensively utilized due to their strong mechanical properties, lightweight design, ease of manufacturing, and adaptability to both flat and curved surfaces. Additionally, they can support dual and triple frequency operations. For wearable applications, it is crucial to ensure that the antenna poses no harm to the human body while still performing effectively at higher frequencies. In this paper, a microstrip patch antenna was developed to operate in the 5.8 GHz ISM band, specifically targeting wearable use cases. To suit wearable environments, Teflon was chosen as the substrate material due to its low dielectric constant ($\varepsilon_r = 2.1$), which contributes to better antenna performance. Simulation results from HFSS 2024 revealed a return loss of –32.93 dB, maximum radiation intensity of 496.31 mW/sr, VSWR of 1.4562, gain of 8 dB, and directivity of 8.543 dB, with an overall efficiency of 87.8%. After fabrication, measurements showed a return loss of –30.843 dB, VSWR of 1.0562, and a measured gain of 12.4 dB. These results indicate that the proposed antenna design is not only efficient but also well-suited for wearable devices operating at 5.8 GHz.

Keywords: ISM Band, Teflon Substrate, Return Loss, VSWR, Antenna Gain, Radiation Efficiency, Directivity, Wireless Body Area Network (WBAN).

ARTICLE INFORMATION

Author(s): Sivasankari Narasimhan, Ashwini G, and Karthika K;
Received: 23/06/25; **Accepted**: 15/12/25; **Published**: 10/03/26;
E- ISSN: 2347-470X;
Paper Id: IJEER250123;
Citation: 10.37391/ijeer.140101
Webpage-link:
https://ijeer.forexjournal.co.in/archive/volume-14/ijeer-140101.html

Publisher's Note: FOREX Publication stays neutral with regard to jurisdictional claims in Published maps and institutional affiliations.

1. INTRODUCTION

The frequency bands within the ISM spectrum are primarily allocated for industrial, scientific, and medical applications, in addition to short-range communication. A key feature of ISM bands is that communication devices operating within these frequencies must tolerate interference generated by ISM equipment. Common ISM bands include 0.9 GHz, 2.4 GHz, and 5 GHz. Antennas operating in the 902–928 MHz range—such as Yagi antennas—are widely used in wireless internet systems, industrial automation, and general ISM applications. Similarly, 2.4 GHz antennas are employed in fabrication, scientific instrumentation, and biomedical monitoring. The 5.8 GHz ISM band (often referred to as HyperLAN) supports numerous applications, including biomedical sensing, high-speed wireless communication, and emergency response systems. For this work, the 5.8 GHz ISM band is selected due to its ability to support high data rates over short ranges, despite its relatively lower penetration depth compared to lower-frequency bands.

When an antenna is placed on the human body, polarization and surface proximity may influence both the propagation path and biological exposure. To minimize the typical 3 dB efficiency loss, monopole antennas are traditionally positioned approximately 30 mm above the skin. Hall et al. [1] demonstrated such a design using a polystyrene substrate (εr = 2.4–2.7) with a gain of 10 dB at 2.45 GHz. Flexible wearable antennas have gained significant interest because of their ability to integrate seamlessly with the human body. Due to its chemical stability and low dielectric constant (εr = 2.67–3.0), polydimethylsiloxane (PDMS) is considered an effective substrate material, as shown by Lin et al. [2]. Materials such as SU-8 require both low dielectric constant and low loss tangent for wearable applications. When an antenna is bent, the increased curvature typically raises the resonant frequency due to increased capacitance, while inductance remains nearly unchanged. A design utilizing such effects operates in the 6.2–6.4 GHz band with a gain of 2.17 dB and approximately 3% efficiency.

High-quality flexible conducting and dielectric materials further expand the range of suitable substrates for wearable antennas. Jiang et al. [3] fabricated PDMS–AgNW composites (εr = 2.67–3.0, loss tangent 0.01–0.05) using the split-post dielectric resonator technique over frequencies from 1 to 5 GHz.

FOREX Publication
Open Access | Rapid and quality publishing
International Journal of Electrical and Electronics Research (IJEER)
Research Article | Volume 14, Issue 1 | Pages 1-9 | e-ISSN: 2347-470X

Hertleer et al. [4] introduced flexible foam substrates offering uniform and stable thickness that remain unaffected under bending or compression. For adequate bandwidth, a substrate thickness of at least 2 mm is recommended. These designs can be incorporated into firefighter uniforms and other wearable systems, operating at 230 MHz with a gain of <6 dB. In a related work, Hertleer et al. [5] developed flexible polymer-based aperture-coupled patch antennas (ACPA) with electro-textile patch and ground layers and non-conductive textile substrates and feed lines. This design operates at 2.4 GHz with a high gain of 20 dB.

Ayd et al. [6] proposed a cotton-substrate monopole for wearable communication, while Kaivanto et al. [7] addressed battery-constrained satellite-wearable systems using Iridium substrates. Rais et al. [8] introduced a suspended-plate antenna configuration suitable for both ISM and HyperLAN bands. Atanasova et al. [9] developed an ultra-compact textile antenna on denim, achieving a bandwidth of 285 MHz (2.266–2.551 GHz), radiation efficiency exceeding 12% in free space (>6% on phantom), and a low 10-g SAR of 0.15 W/kg.

Soontornpipit et al. [10] applied genetic algorithms to design "waffle-type" microstrip patches optimized for the 402–405 MHz MICS band, suitable for cardiac pacemakers. Their study also examined GA optimization strategies, highlighting how feed-position constraints and directional growth biases affect convergence rates. Liu et al. [11] introduced thin low-loss nanocomposite substrates and superstrates for dual-band implantable antennas with enhanced bandwidth and radiation efficiency. Additional spiral resonators broaden the bandwidth in the MICS band. Both spiral and serpentine geometries, explored by Soontornpipit et al. [12], offer reduced size compared to conventional patches, with spiral structures being the more compact option. For implantable designs, biocompatible materials with low conductivity and relatively thicker superstrates are preferred. This paper presents the design of a wearable antenna operating at 5.8 GHz for ISM-band applications. The proposed antenna offers several novel advantages:
(i) a compact form factor optimized for wrist-mounted operation;
(ii) simultaneous optimization for low Specific Absorption Rate (SAR) and high radiation efficiency, ensuring safe and effective long-term use on the human body; and
(iii) satisfactory performance in terms of return loss, directivity, and overall efficiency.

The remainder of the paper is organized as follows: *Section 2* describes the proposed wearable antenna design, *section 3* discusses the results and design rationale, and *section 4* concludes the work.

2. DESIGN OF WEARABLE PATCH ANTENNA

The main aim for designing the proposed antenna is to make it useful for wearable applications. The operating frequency is preferred in the ISM band with a higher frequency band gap of 5.725-5.875 GHz. For communication to RFID applications the gain should be above 3 dB with directivity between 5-7 dB. In addition to that, this design is aimed at less specific absorption rate which is less than 1.6 W/Kg as per the IEEE standards for radiation effects Tak et al. [16].

2.1. Patch Antenna for Wearable Applications

The substrates having lesser dielectric constant provide flexibility, here, the substrate Teflon is used. The properties of the substrate are shown in *table 1*. Almost the characteristics of Teflon match with the wearable-body characteristics.

Table 1. Teflon characteristics

Property	Values	Units
Impact Strength	$1.5e^4$ - $1.7e^4$	J/m^2
Insulator or Conductor property	Insulating property	
Specific Heat Capability	970 - $1.09e^3$	J/kg °C
Melting Temperature	315 - 339	°C

The proposed microstrip patch antenna is designed to be flexible and wrapped around the wrist, enabling use in wearable applications that accommodate all hand movements. To improve gain and efficiency, slots have been introduced into the patch. A 50Ω transmission line configuration ensures proper impedance matching.

Six antenna designs, labeled *A* through *F*, were simulated to identify the best-performing model, as shown in *figure 3*. Each design was evaluated based on gain, directivity, Specific Absorption Rate (SAR), efficiency, and return loss to ensure accurate results in terms of SAR and polarization. The dimensions for all designs, determined by initial design equations and refined through parametric analysis, are summarized in *table 2*. Design *A* features a significantly larger ground plane and substrate compared to Designs *B* through *F*, which have similar ground plane sizes. Design *D* stands out with a higher effective dielectric constant and larger patch dimensions. Among all, Design *F* exhibits the best overall performance in gain, return loss, and efficiency. *Figures 4* and *5* present the detailed schematic and cross-sectional views of Design *F*, showcasing its finalized dimensions and layered structure.

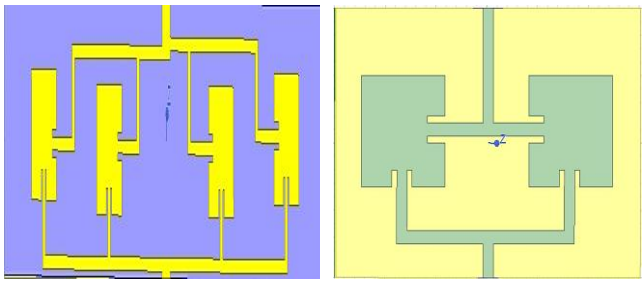

Design A Design B

FOREX Publication
Open Access | Rapid and quality publishing
International Journal of Electrical and Electronics Research (IJEER)
Research Article | Volume 14, Issue 1 | Pages 1-9 | e-ISSN: 2347-470X

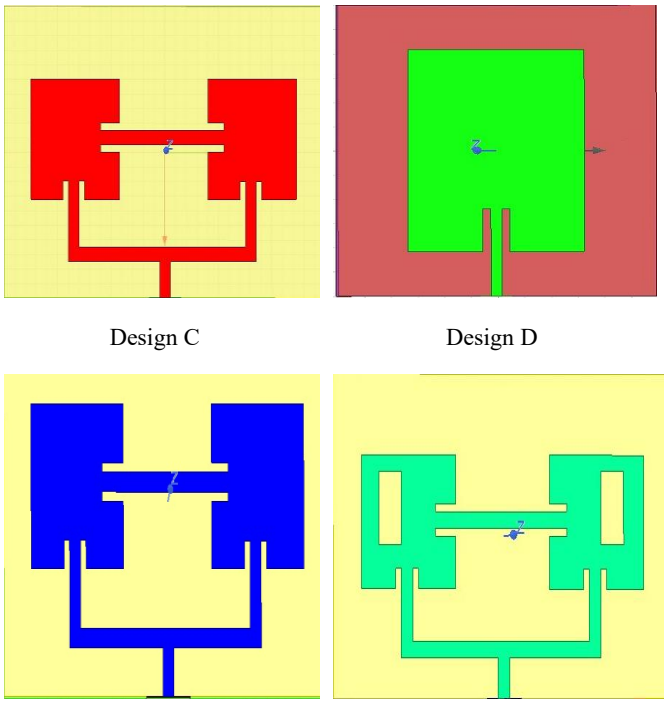

Figure 1. Design of Wearable Patch antennas

The dimensions of the Designs are obtained from the design equations and are finalized by using the parametric analysis from the project manager as shown in *table 2*.

To check the antenna for wearable usages, a human hand model from ANSYS has been used in this paper which is shown in *figure 3*. This model is used for checking the Specific Absorption Rate (SAR) and radiation effect in the human body, from the HFSS software. Over the hand prototype, the antenna with dimensions given in *figure 3* is placed to observe the results.

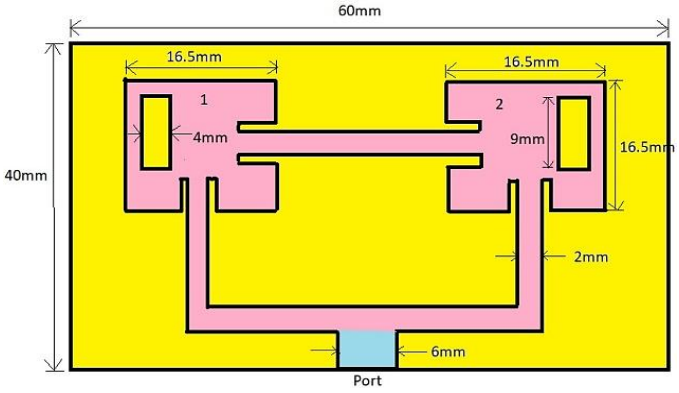

Figure 2. Antenna Design F measurements

Table 2. Return loss for various design

Design Name	A	B	C	D	E	F
Return Loss (dB)	17.1	9.62	20.6	7.7	17.4	32.9
Frequency (GHz)	6.67	5.85	5.23	4.53	6.27	5.80

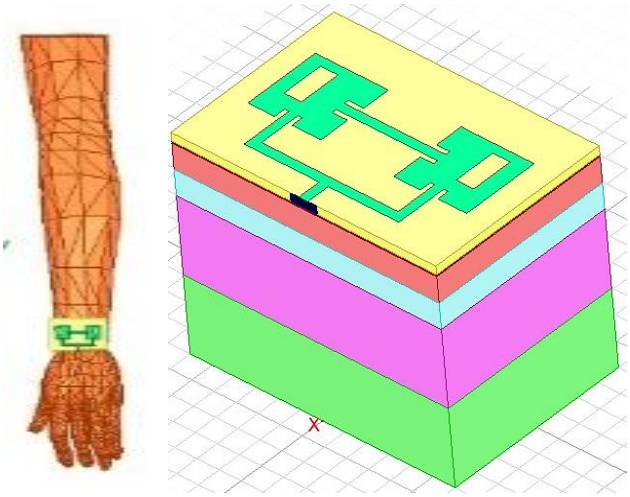

Figure 3. Antenna design with Phantom model

Exact specifications used for introducing the phantom model like that of Human hand Paraskevopoulos et al. [17] are as shown in *table 3*.

Table 3. Human Phantom Design parameters

Color Indications	Human Part	Thickness	Permittivity	Conductivity
Green	Bone	15	9.7	1.16
Pink	Muscle	15	48.4	4.92
Blue	Fat	5	4.85	0.33
Red	Dry Skin	5	35.2	3.72

3. RESULTS AND DISCUSSION

All the design parameters are simulated in HFSS software. This section, elaborately discusses the simulation results of antenna implemented in hand.

Figure 4. Proposed model as hand band

FOREX Publication
Open Access | Rapid and quality publishing
International Journal of Electrical and Electronics Research (IJEER)
Research Article | Volume 14, Issue 1 | Pages 1-9 | e-ISSN: 2347-470X

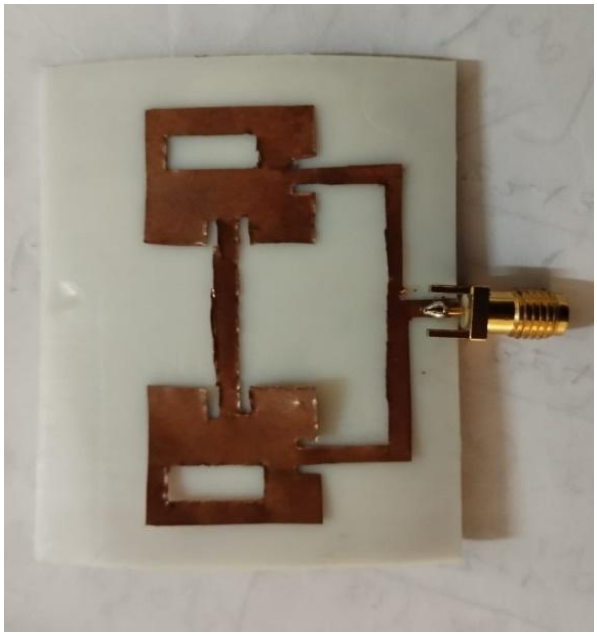

Figure 5. Implemented prototype

3.1. Return Loss

Return Loss (RL) is the ratio of the reflected power to the incident (input) power, expressed in decibels.

$$\text{Return loss} = —20 \log |\Gamma| \quad (1)$$

High return loss (*e.g.*, 20 dB or more) indicates good matching, very little signal is reflected. Low return loss (*e.g.*, below 10 dB) indicates poor matching, where significant reflection occurs.

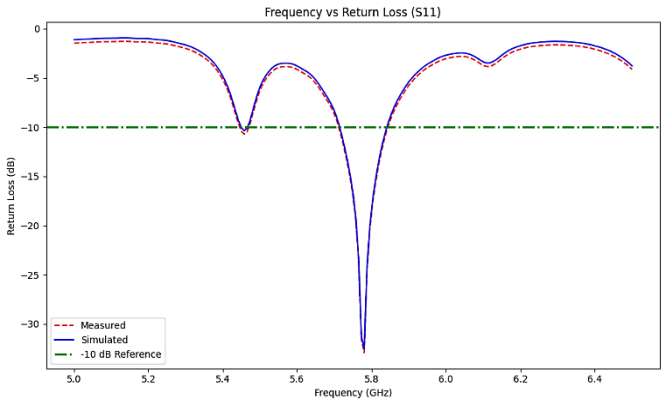

Figure 6. Return loss from the proposed design

Figure 6 shows that the return loss of the antenna remains almost same at the operating frequency of 5.79 GHz. Its return loss is -32.93 dB. From *figure 6*, it is inferred that, both simulated and measured prototype results are aligned in the same return loss curve. Then the proposed design is tested with phantom model and its return loss is plotted in *figure 7*.

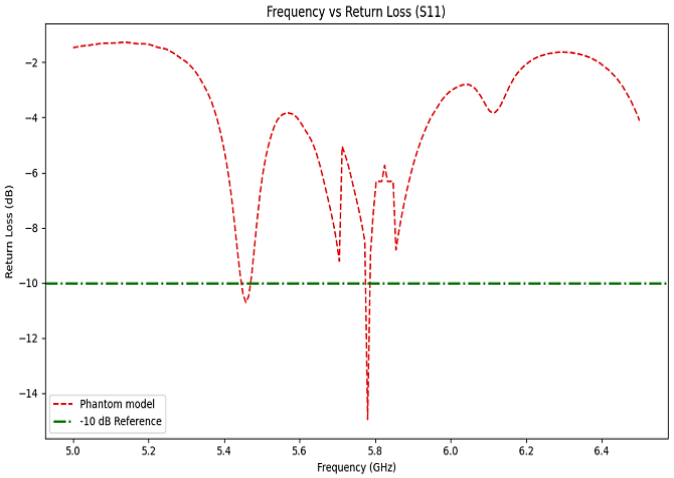

Figure 7. Phantom model return loss

shows that the return loss of the antenna remains almost same at the operating frequency of 5.79 GHz. From *figure 7*, its return loss is -14.8001 dB. It mostly aligns with the return loss of the prototype model.

3.2. Radiation Plots

Radiation pattern gain represents how effectively an antenna directs radiated power in a specific direction compared to an isotropic radiator. Higher gain indicates stronger signal concentration in that direction, improving communication range and performance.

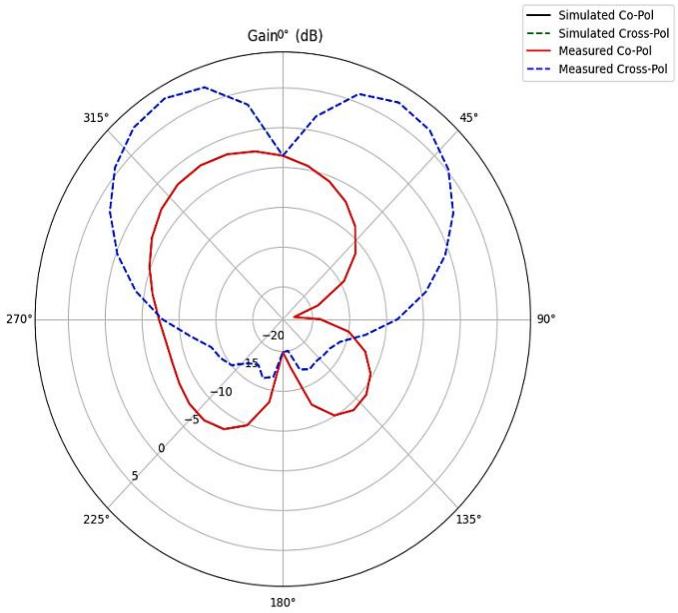

Figure 8. *2-D*imensional gain of antenna

Figure 8 shows the Radiation pattern of the antenna model, where the radiation is obtained in all the omni directions from -30 degree to 30 degree.

FOREX Publication
Open Access | Rapid and quality publishing
International Journal of Electrical and Electronics Research (IJEER)
Research Article | Volume 14, Issue 1 | Pages 1-9 | e-ISSN: 2347-470X

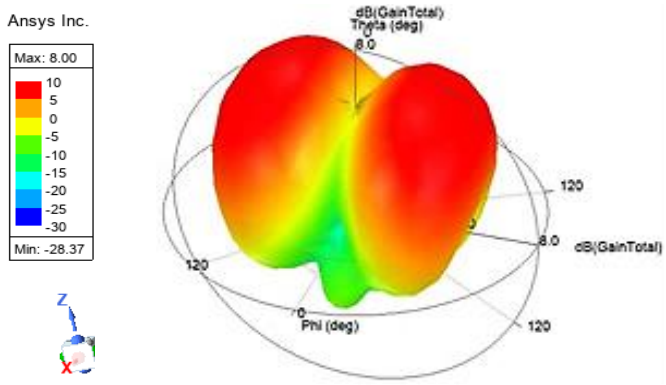

Figure 9. *3-D*imension gain plot

Maximum of 8 dB has been achieved as shown in Figure 9. Phantom model gain also shows 7.6 dB maximum gain which is depicted in *figure 10*, which ranges from -85 degree to 85 degree.

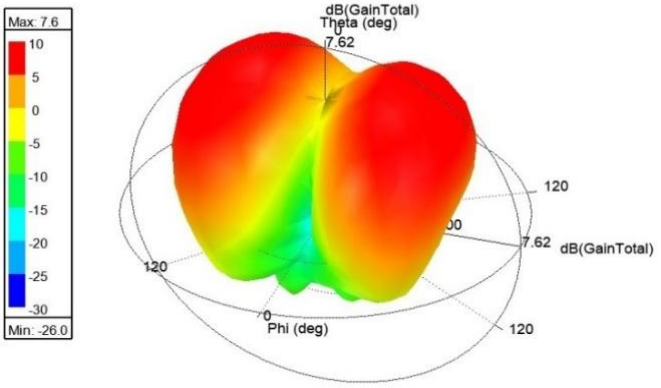

Figure 10. *3-D*imensional gain plot for phantom model

Hence it can be inferred that the antennas having gain greater than 3 dB from the simulated design are suitable for wearable applications.

3.3. Electric-Magnetic Field Distribution

The electric field distribution plays a critical role in determining antenna performance, especially when placed close to the human body. In wearable environments, the field must be controlled to minimize tissue exposure while ensuring efficient radiation. A uniform and well-confined electric field around the patch enhances impedance matching and stability during bending or movement. The interaction between the electric field and biological tissues can affect SAR levels, making low-dielectric, bio-compatible materials essential. In this design, as shown in *figure 11*, maximum of 7500 V/m vector potential is only obtained from this design.

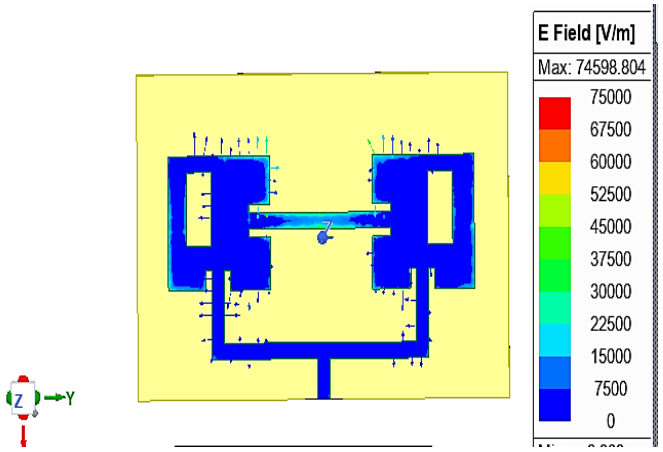

Figure 11. Electric field distribution

Similarly, the magnetic field, which is orthogonal to the electric field is shown in *figure 12*.

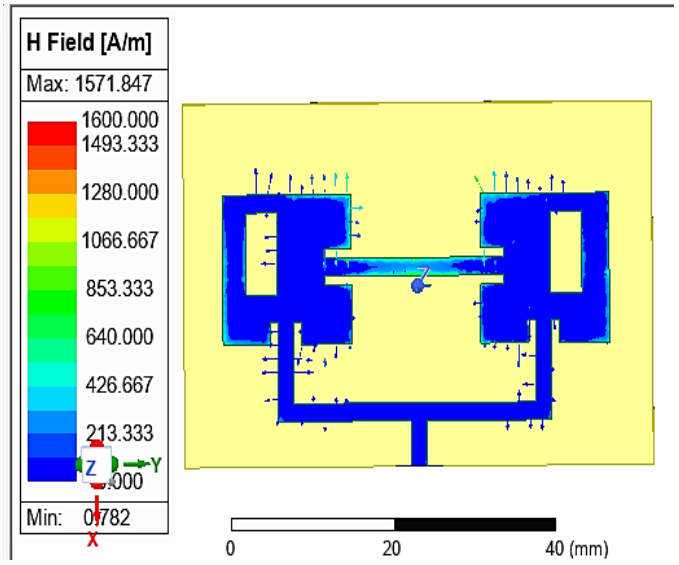

Figure 12. Analysis of magnetic field

Maximum magnetic field intensity for this design is 426.667 A/m. *table 4* lists out some key parameters such as Resonant frequency, return loss, Directivity, Gain Efficiency Radiation intensity, radiated power and Front to back ratio of the antenna and Phantom model with antenna are extracted to study the effects of proximity to human tissue. Simple Antenna SAR results are given in *figure 13*. Anechoic chamber measurement setup for the proposed antenna is shown in *figure 14*. Here Corrugated horn antenna is set up as the reference antenna. From *table 4*, it can be inferred that the antenna and its phantom models are aligned in radiation intensity and gain properties. Other parameters varying by 10-15% Some of the relevant works with wearable antenna applications are given in *table 5*.

FOREX Publication
Open Access | Rapid and quality publishing
International Journal of Electrical and Electronics Research (IJEER)
Research Article | Volume 14, Issue 1 | Pages 1-9 | e-ISSN: 2347-470X

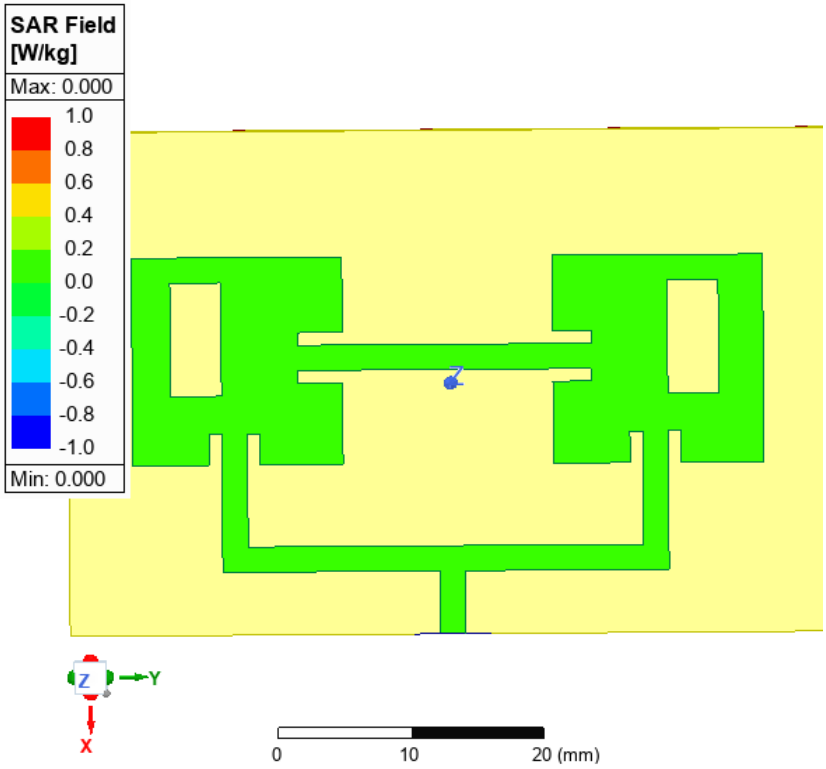

Figure 13. SAR field analysis

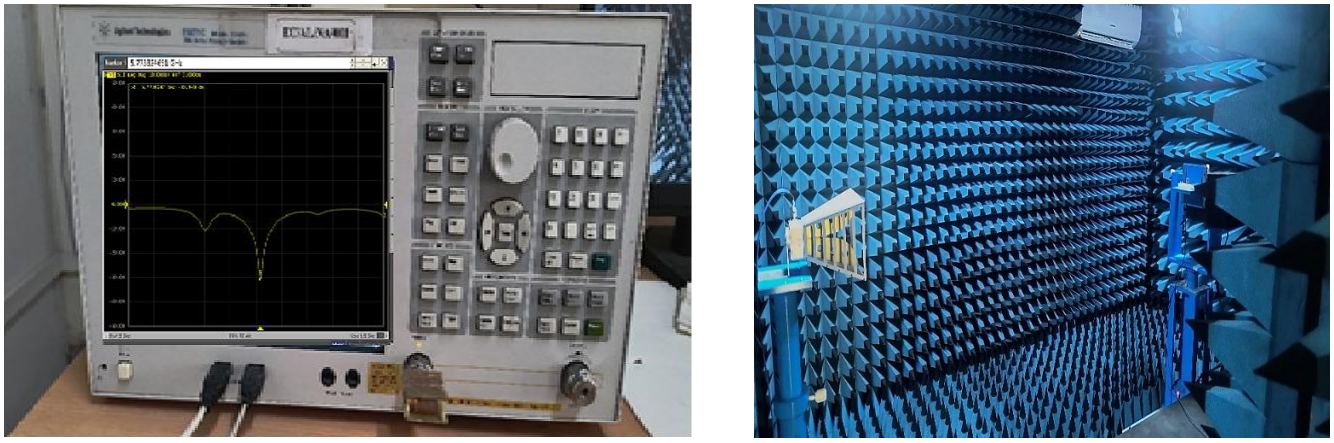

(a) (b)

Figure 14. (a) Return loss set up in Vector network analyzer (b) Anechoic chamber measurement set-up of the proposed antenna

Table 4. Comparison between designed Antenna and phantom model

Design name	Resonant frequency (GHz)	Gain (dB)	Return Loss(dB)	Directivity (dB)	Efficiency η(%)	Radiation Intensity (mW/Sr)	Radiated power (mW)	Front to Back Ratio
Antenna design	5.8	8	32.93	3.1656	87.8	496.31	872.07	284.29
Antenna design with Phantom model	5.8	7.6	14.99	2.2417	83.9	455.24	829.23	58.824

FOREX Publication
Open Access | Rapid and quality publishing
International Journal of Electrical and Electronics Research (IJEER)
Research Article | Volume 14, Issue 1 | Pages 1-9 | e-ISSN: 2347-470X

Table 5. Comparison with Previous works

Ref No.	Name of the Substrate used	Dimensions	Gain	Efficiency	Frequency
Hall et al. [1]	Polystyrene	ground 50*50*0.4mm, patch :31*0.5mm substrate thickness=9mm,	10dB	40-50%	2.45GHz
Lin et al. [2]	Polydimethylsiloxane PDMS	ground plane:46.4*20mm, patch :14.4*17.36mm, substrate thickness:500μm	2.17dB	-	6.2-6.4GHz
Jiang et al. [3].	Composite mixture of PDMS and AgNWs (Silver nanowires)	ground plane:50*50mm, patch :21*21mm, substrate thickness:3.5mm	5.2dB	76-79%	2.4GHz
Hertleer et al. [4]	Shock Absorbing foam	ground plane:50*46mm, patch :9*7mm, substrate thickness:8mm	<6dB	-	230MHz
Hertleer et al. [5]	Flexible polymer	ground plane:5.2*14.5mm, patch :49*61.6mm, substrate thickness:2.56mm	20dB	63%	2.4GHz
Ayd et al. [6]	Polydimethylsiloxane & PDMS	ground plane:37*37*0.1mm, patch :20*24*0.1mm, substrate thickness:1mm	35dB	~90%	3.0 to 4.0 GHz
Kaivanto et al. [7]	Cordura and Woven fabric	ground plane:65*65mm, substrate thickness:3mm	-2.5 to +7.5dB	65%	1575MHz & 1621.35-1626.50MHz
Rais et al. [8]	Polyurethane foam (εr = 0.1)	ground plane:100*80mm, patch :60*45mm substrate thickness:5mm	8.33dB	67%	227MHz & 850MHz
Atanasova et al. [9]	RT/Duriod 5880 (εr = 2.2)	ground plane:24*12*6mm, patch :0.254*0.787mm	25dB	85, 82, 80%	9.6, 14.8 & 34.5 GHz
Soontornpipit et al. [10]	RT/Duriod 6002	Each cell is 1 mm, total size is28*24 mm^2. The feed point is 19 mm2 mm^2, ground point is 8 mm* 2 mm	-	-	402–405 MHz
Liu et al. [11]	Rogers 3010	ground plane:16.5mm, substrate:17.5mm, patch dimensions is 16.5*16.5*2.54 mm^3	30dB at 402MHz & 31.5 dB at 430 MHz	-	402-430MHz
Soontornpipit et al. [12]	Macor, Teflon (or)Ceramic Alumina	substrate thickness:3mm, antenna is centered in a 50*40*20 mm	-	-	402 and 475 MHz
Anand et al. [18]	FR4 epoxy	Substrate thickness: 1.6mm	7.74dB	-	6.65 – 13.85GHz
Indumathi et al. [19]	Cordura Fabric	Ground plane: 28*60mm, substrate:0.57mm, radius of patch: 14mm	3.2dB	-	2 to 9.6GHz
Anand and Palnila Devi [20]	FR4 epoxy	ground plane:23*23mm, patch element:12.5*17.5mm; substrate thickness:1.6mm	20dB	-	1.98 to 3.59 GHz
Kingsta et al. [21]	FR4 epoxy	Overall dimension: 55*30.735mm substrate thickness:1.6mm	9.9386dB	-	5.85 to 5.925 GHz
Renuga Kanni and Brinda [22]	FR4 epoxy	Overall dimension: 20.2*24.1*1.6mm3	4.71dB	78%	5.85 to 5.925 GHz
Viswanadha, and Raghava [23]	RO-4003C	Overall dimension: 10*6.5*0.035mm3	3.2dB at 6.8GHz, 5.42 dB at 9.5GHz & 5.56dB at 9.89GHz	82.1% at 6.8GHz, 86.3% at 9.5GHz &88.1% at 9.89GHz	6.8GHz
Ghasemlouy, and Rajebi [24]	FR4 epoxy	Ground plane: 70.51*45.33mm, substrate: 0.7mm, patch dimension: 62*41 mm	-	-	2.24 GHz
Kushwaha, and Chauhan [25]	FR4 epoxy	Substrate thickness: 1.57mm	6.27dB	-	18.8GHz

International Journal of Electrical and Electronics Research (IJEER)
Research Article | Volume 14, Issue 1 | Pages 1-9 | e-ISSN: 2347-470X

Yadav,and Mishra [26]	FR4 epoxy	Ground plane: 10*40mm, substrate: 1.59mm	-	-	2 to 13.2 GHz
Prajapati et al. [27]	Roger RT/duroid 5880(tm)	substrate: 3.2mm, patch dimension: 38*29 mm	-	-	2.4654 to 2.5158 GHz
Proposed	Teflon	substrate: 40x 60 mm; Patch dimensions 16.5 x16.5 mm (2 times)	32.93 dB	87.85 %	5.79 GHz.

Table 6. Comparison with Other Wearable Antenna

Antennas	Feed Method	No. of Ports	Polarization	Radiation Efficiency	Operating Frequency
Soontornpipit et al. [12]	Probe	1	LP	-	402 MHz
Werner et al. [13]	Microstrip	2	Dual LP	90%	5.8GHz
Salonen et al. [14]	Probe	1	LP	40%	2.4GHz
Wang et al. [15]	Probe	1	LP	-	3.3-3.4GHz
Proposed	Microstrip	1	LP	87.8%	5.8GHz

Table 6 shows the comparison of the proposed antenna for polarization and efficiency. Simulation and measurement results confirm that the proposed wearable antenna resonates accurately at 5.8 GHz with good impedance matching, achieving a measured return loss of -32.93 dB depending on placement conditions. The antenna maintains a usable −10 dB impedance bandwidth of approximately 5.75-5.85 GHz, sufficient to fully cover the 5.8 GHz ISM band. The antenna demonstrates a realized gain ranging from 7.6 dB in on-body configuration indicating minimal degradation due to body proximity. Specific absorption rate (SAR) analysis reveals that only 0.02 W/kg only obtained which is well below FCC and ICNIRP safety limits, indicating that the antenna is suitable for safe long-term wearable use.

4. CONCLUSION

The developed microstrip patch antenna exhibits excellent suitability for wearable applications in the 5.8 GHz ISM band, combining high efficiency, compact dimensions, and strong mechanical flexibility. The incorporation of a Teflon substrate significantly enhanced the radiation characteristics and ensured stable on-body performance. Both simulated and measured results showed close agreement, with notable improvements in return loss, VSWR, and gain, thereby validating the robustness and reliability of the proposed design. Overall, this antenna offers a high-performance and practically viable solution for next-generation wearable wireless communication systems, particularly in IoT, healthcare, and biomedical monitoring environments.

Acknowledgments: Our thanks to the experts who have contributed towards this work and Mepco Schlenk Engineering college ECE department members.

Conflicts of Interest: Authors stated that no conflict of Interest.

REFERENCES

[1] P. S. Hall et al., 2007 “Antennas and propagation for on-body communication systems,” IEEE Antennas Propag. Mag., vol. 49, no. 3, pp. 41-58, Jun. 2007.

[2] C. P. Lin, C. H. Chang, Y. T. Cheng, and C. F. Jou, 2011 “Development of a flexible SU-8 PDMS-based antenna,” IEEE Antennas Wireless Propag. Lett., vol. 10, pp. 1108-1111.

[3] Z. H. Jiang, Z. Cui, T. Yue, Y. Zhu, and D. H. Werner,2017 “Compact, highly efficient, and fully flexible circularly polarized antenna enabled by silver nanowires for wireless body area networks,” IEEE Trans. Biomed. Circuits Syst., vol. 11, no. 4, pp. 920-932.

[4] C. Hertleer, H. Rogier, L. Vallozzi, and L V. Langenhove, 2009 “A textile antenna for off-body communication integrated into protective clothing for fire Fighters,” IEEE Trans. Antennas Propag., vol. 57, no. 4, pp. 919-925.

[5] C. Hertleer, A. Tronquo, H. Rogier, L. Vallozzi, and L. V. Langenhove, 2007 “Aperture-coupled patch antenna for integration into wearable textile systems,” IEEE Antennas Wireless Propag. Lett., vol. 6, pp. 392-395, 2007.

[6] Ayd R. Saad, Ayman, Walaa M. Hassan, and Ahmed A. Ibrahim. 2023. "A monopole antenna with cotton fabric material for wearable applications." Scientific Reports 13, no. 1 (2023): 7315.

[7] E. K. Kaivanto, M. Berg, E. Salonen, and P. D. Maagt, 2011. “Wearable circularly polarized antenna for personal satellite communication and navigation,” IEEE Trans. Antennas Propag., vol. 59, no. 12, pp. 4490-4496.

[8] N. M. S. Rais, P. J. Soh, M. F. A. Malek, and G. E. Vanden bosch 2013 “Dual-band suspended-plate wearable textile antenna,” IEEE Antennas Wireless Propag. Lett., vol. 12, pp. 583-586, 2013.

[9] Atanasova, G., & Atanasov, N. 2020. Small Antennas for Wearable Sensor Networks: Impact of the Electromagnetic Properties of the Textiles on Antenna Performance. Sensors, 20(18), 5157.

[10] P. Soontornpipit, C. M. Furse and You Chung Chung, 2005 "Miniaturized biocompatible microstrip antenna using genetic algorithm," in IEEE Transactions on Antennas and Propagation, vol. 53, no. 6, pp. 1939-1945.

[11] C. Liu, Y. -X. Guo and S. Xiao. 2012 “Compact Dual-Band Antenna for Implantable Devices," in IEEE Antennas and Wireless Propagation Letters, vol. 11, pp. 1508-1511.

[12] P. Soontornpipit, C. M. Furse and You Chung Chung, 2004. "Design of implantable microstrip antenna for communication with medical implants," in IEEE Transactions on Microwave Theory and Techniques, vol. 52, no. 8, pp. 1944-1951.

[13] D. H. Werner and Z. H. Jiang, 2016 Electromagnetics of Body Area Networks: Antennas, Propagation, and RF Systems, Wiley-IEEE Press.

[14] P. Salonen, and Y. Rahmat-Samii, 2015 “Textile antennas: Effects of antenna bending on input matching and impedance bandwidth,” IEEE A&E Systems Magazine., vol. 22, no. 12, pp. 18-22.

International Journal of
Electrical and Electronics Research (IJEER)
Research Article | Volume 14, Issue 1 | Pages 1-9 | e-ISSN: 2347-470X

[15] Z. Wang, L. Lee, D. Psychoudakis, and J. Volakis.2014 "Embroidered multiband body-worn antenna for GSM PCS WLAN communications," IEEE Trans. Antennas Propag., vol. 62, no. 6, pp. 3321-3329, Jun. 2014.

[16] J. Tak, Y. Hong, and J. Choi,2015 "Textile antenna with EBG structure for body surface wave enhancement," Electron. Lett., vol. 51, pp. 1131-1132.

[17] A. Paraskevopoulos, D. S. Fonseca, R. D. Seager, W. G. Whittow, J. C. Vardaxoglou, and A. A. Alexandridis, 2016 "Higher-mode textile patch antenna with embroidered vias for on-body communication," IET Microw. Antennas Propag., vol. 10, no. 7, pp. 802-807.

[18] Anand Swaminathan, Josephine Pon Gloria Jeyaraj, Ahila G, Afrin A, 2020 "RCS reduction using a wideband dual logarithmic step patch PRRM in microstrip patch antenna", Microwave and Optical technology Letters, VOL. 63, Issue 1.

[19] G. Indumathi and Bhavithra J. 2017. "Wearable textile antenna for indoor applications," 2017 International Conference on Inventive Communication and Computational Technologies (ICICCT), 2017, pp. 30-34.

[20] Anand, S. and Palniladevi, P. 2020 'Dynamic enhanced proximity coupling technique for antennas', Int. J. Wireless and Mobile Computing, Vol. 18, No. 3, pp.233–241.

[21] R. M. Kingsta and Seyatha K 2019."Design and Performance Comparison of Metamaterial Superstrate Antenna for DSRC Applications," 2019 3rd International Conference on Trends in Electronics and Informatics (ICOEI), 2019, pp. 1-6.

[22] V. Renuga Kanni and R. Brinda, 2019. "Design of High Gain Microstrip Antenna for Vehicle-to-Vehicle Communication Using Genetic Algorithm," Progress in Electromagnetics Research M, Vol. 81, 167-179.

[23] Viswanadha, K., Raghava, N.S. 2020 "Design and Analysis of a Compact Dual-Band Serpentine-Shaped Patch Antenna with Folded Stub Lines for C- and X-Band Applications. J. Commun. Technol. Electron. 65, 1147–1160.

[24] Ghasemlouy, A., Rajebi. 2019. S. Investigation and Evaluation of the Effect of Silicon Layer and Its Comparison with Water Bolus in Designing Microstrip Antenna for Hyperthermia Applications. J. Commun. Technol. Electron. 64, 1307–1317.

[25] Kushwaha, R., Chauhan, R.K. 2019. "Dual Band Slotted Patch Microstrip Antenna Array Design for K Band Application" In: Verma, S., Tomar, R., Chaurasia, B., Singh, V., Abawajy, J. (eds) Communication, Networks and Computing. CNC 2018. Communications in Computer and Information Science, vol 839. Springer, Singapore.

[26] Yadav, R., Mishra, R. 2020. Microstrip Patch Antenna Array for UWB Application. In: Janyani, V., Singh, G., Tiwari, M., d'Alessandro, A. (eds) Optical and Wireless Technologies. Lecture Notes in Electrical Engineering, vol 546. Springer, Singapore.

[27] Prajapati, M.S., Rawat, A., Parikh, R., Joshi, P. 2019. "Analysis of Impact of Circular Cut on Microstrip Patch Antenna at 2.49 GHz for S Band Application. In: Nath, V., Mandal, J. (eds) Proceedings of the Third International Conference on Microelectronics, Computing and Communication Systems. Lecture Notes in Electrical Engineering, vol 556. Springer, Singapore.